

# Unsteady Thermal Blooming of Intense Laser Beams

J. T. ULRICH AND P. B. ULRICH

*Optical Sciences Division*

January 31, 1980



**NAVAL RESEARCH LABORATORY**  
**Washington, D.C.**

Approved for public release; distribution unlimited.

SECURITY CLASSIFICATION OF THIS PAGE (When Data Entered)

REPORT DOCUMENTATION PAGE		READ INSTRUCTIONS BEFORE COMPLETING FORM
1. REPORT NUMBER NRL Report 8352	2. GOVT ACCESSION NO.	3. RECIPIENT'S CATALOG NUMBER
4. TITLE (and Subtitle) UNSTEADY THERMAL BLOOMING OF INTENSE LASER BEAMS		5. TYPE OF REPORT & PERIOD COVERED Final report 1975-1977 on one phase of a continuing NRL problem number
		6. PERFORMING ORG. REPORT NUMBER
7. AUTHOR(s) J. T. Ulrich and P. B. Ulrich		8. CONTRACT OR GRANT NUMBER(s)
9. PERFORMING ORGANIZATION NAME AND ADDRESS Naval Research Laboratory Washington, D.C. 20375		10. PROGRAM ELEMENT, PROJECT, TASK AREA & WORK UNIT NUMBERS NRL Problem R05-31
11. CONTROLLING OFFICE NAME AND ADDRESS Naval Sea Systems Command, PMS-405 Washington, D.C. 20362		12. REPORT DATE January 31, 1980
		13. NUMBER OF PAGES 18
14. MONITORING AGENCY NAME & ADDRESS (if different from Controlling Office)		15. SECURITY CLASS. (of this report) UNCLASSIFIED
		15a. DECLASSIFICATION/DOWNGRADING SCHEDULE
16. DISTRIBUTION STATEMENT (of this Report) Approved for public release; distribution unlimited.		
17. DISTRIBUTION STATEMENT (of the abstract entered in Block 20, if different from Report)		
18. SUPPLEMENTARY NOTES		
19. KEY WORDS (Continue on reverse side if necessary and identify by block number) Thermal blooming Laser propagation Atmospheric propagation High power lasers		
20. ABSTRACT (Continue on reverse side if necessary and identify by block number) A four-dimensional (three space plus time) computer program has been written to compute the nonlinear heating of a gas by an intense laser beam. Unsteady, transient cases are capable of solution and no assumption of a steady state need be made. The transient results are shown to asymptotically approach the steady-state results calculated by the standard three-dimensional thermal blooming computer codes. The report discusses the physics of the laser-absorber interaction, the numerical approximation used, and comparisons with experimental data. A flowchart is supplied in the appendix to the report.		

## CONTENTS

INTRODUCTION .....	1
PHYSICS OF THE LASER-FLUID INTERACTION.....	2
COMPUTATIONAL DETAILS.....	4
FREE CONVECTION.....	6
SOURCES OF ERROR.....	8
COMPARISON WITH EXPERIMENT.....	10
CONCLUSIONS .....	14
REFERENCES .....	14
APPENDIX -- Flowchart.....	15

## UNSTEADY THERMAL BLOOMING OF INTENSE LASER BEAMS

## INTRODUCTION

When laser light passes through an absorbing fluid, the beam intensity is reduced by molecular absorption. If the fluid contains inhomogeneities or impurities (for example, particulate matter or turbulent eddies in the case of a gas) other scattering and absorption mechanisms can contribute to intensity reduction. This report is confined to a study of laser beam propagation through an absorber for which it is appropriate to describe the interaction of the light and the fluid by means of an absorption constant per unit length of absorbing path. At low powers a single absorption constant  $\alpha$  suffices to describe the beam diminution even in the presence of scattering centers. At high powers, however, the absorbed energy causes significant enough alteration of the ambient fluid density that the light beam itself is perturbed, not simply diminished. This phenomenon of self-distortion of the coherent phase front due to absorber heating is called thermal blooming. If scattering is occurring as well, then it is important to separate the purely "elastic" losses of the beam via scattering from the "inelastic" losses via absorption so that the absorption coefficient is written

$$\alpha = \alpha_{scatt} + \alpha_{abs}.$$

Thermal blooming has been studied under a variety of limiting conditions. If a wind is present in the absorbing gas, or if the beam itself is moving through the fluid, then the heated volume of the absorber is removed from the beam path after residing a finite time (about equal to beam size/fluid speed relative to the beam) and a steady state can evolve. Time no longer explicitly enters the problem and a three-space-dimensional analysis is appropriate. The resultant nonlinear problem has been studied exhaustively at NRL and a number of other laboratories. [1] Another limit of interest is the regime of times which is much shorter than the wind transit time across the beam. Then, if the initial beam is distributed symmetrically about the propagation axis, the thermal blooming evolves symmetrically about the propagation axis, the thermal blooming evolves symmetrically and, again, just three coordinates are needed: the radius, the range, and time. This regime also has been studied. [1]

There are, however, other space-time regimes of interest and importance in naval applications of high-energy lasers, such as arbitrary (noncircularly symmetric) aperture distributions in the short-time regime, arbitrary distributions in the regime before steady state is attained, propagation through wind-null points in the beam path, propagation of time-varying aperture distributions, and multiple pulse train propagation. These require a four-dimensional analysis.

This report details the development of a four-dimensional computer program which is being used to study the preceding problems. The physics of the light beam, the fluid, and their interaction are discussed. A section is devoted to some numerical details, a comparison with some experimental data is given, and a flowchart is provided as an appendix.

## PHYSICS OF THE LASER-FLUID INTERACTION

When the laser is first turned on, a transient state evolves during which the temperature of the fluid increases due to local heating at the rate  $\alpha_{abs}I(x, y, z, t)$  ergs per unit volume per unit time, where  $I$  is the laser beam intensity. A pressure wave propagates away from the beam at the speed of sound. Directed velocity of the fluid away from the beam region leads to density decrease there. This study is confined to times after these transients have died out, which times are on the order of the beam size/sound speed. In this limit, as will be shown below, the density changes are proportional to the heat absorbed by a fluid element during its residence in the beam.

The fluid equations to be solved are conservation of mass

$$\frac{D\rho}{Dt} + \rho D \cdot \mathbf{v} = 0; \quad (1)$$

conservation of momentum

$$\rho \frac{D\mathbf{v}}{Dt} + \nabla p = 0, \quad (2)$$

and conservation of energy

$$\rho \frac{\partial \epsilon}{\partial t} + p \nabla \cdot \mathbf{v} = \dot{Q}, \quad (3)$$

where

$$\frac{D}{Dt} \equiv \frac{\partial}{\partial t} + \mathbf{v} \cdot \nabla.$$

In the equations  $\rho$ ,  $\mathbf{v}$ , and  $p$  are the density, velocity, and pressure,  $\epsilon$  is the internal energy per unit volume  $\epsilon = C_V T$ , where  $C_V$  is the specific heat at constant volume per unit volume,  $T$  is the temperature, and  $\dot{Q}$  is the rate of heat deposition by the laser beam per unit volume, so that  $\dot{Q} = \alpha_{abs}I$ .

In the time regime in the preceding discussion pressure is considered constant. In addition, an ideal gas equation of state is assumed. Then Eqs. (1), (2), and (3) become

$$\frac{D\rho}{Dt} = \frac{-\rho}{\Gamma p_o} (\Gamma - 1) \alpha_{abs} I, \quad (4)$$

where  $\Gamma = C_P/C_V$  and  $C_P$  is the specific heat at constant pressure per unit volume, and  $p_0$  is the ambient pressure.

In all cases of interest  $\Delta\rho \sim \theta(\alpha)$  and linearization of the hydrodynamics is performed. This assumption must be checked in some cases (for example, long pulses of high energy in a confined absorption cell can lead to significant temperature changes compared with ambient values [2]). For naval applications, however, the assumption is satisfied very well. Thus,

$$\rho = \rho_0 + \rho_1, \rho_1 \ll \rho_0$$

and Eq. (4) becomes

$$\frac{D\rho_1}{Dt} = -\frac{(\Gamma - 1)}{C_S^2} \alpha_{abs} I, \quad (5)$$

where  $C_S$  is the sound speed,  $\sqrt{\Gamma p_0/\rho_0}$ . The solution to Eq. (5) is

$$\rho_1(\mathbf{r}, z, t) = \frac{-(\Gamma - 1)}{C_S^2} \alpha_{abs} \int_0^t I[\mathbf{r} - \mathbf{v}(t - t')] dt'. \quad (6)$$

This result reduces to some of the limiting cases which were the subject of earlier studies, as will now be shown.

For  $\mathbf{v} = 0$ , and short times (longer, however, than the beam size/sound speed) Eq. (6) becomes

$$\rho_1(\mathbf{r}, z, t) = -(\Gamma - 1)\alpha_{abs} I(\mathbf{r}, z, t)t, \quad (7)$$

which is the density change appropriate to long pulses for which negligible degradation has occurred during the transient sound wave period [3] ( $\mathbf{r} \rightarrow |\mathbf{r}|$  for circularly symmetric initial conditions).

For  $\mathbf{v} \neq 0$  anywhere between aperture and focal point, and for  $t \rightarrow \infty$ , Eq. (6) becomes, with  $\mathbf{r}' = \mathbf{r} - \mathbf{v}(t - t')$

$$\rho_1(\mathbf{r}, z) = \frac{(\Gamma - 1)\alpha_{abs}}{|\mathbf{v}|C_S^2} \int_{-\infty}^{\mathbf{r}} I_{CW}(\mathbf{r}', z) d\mathbf{r}', \quad (8)$$

which is the form of the density changes in the CW propagation studies [4].

In the current study, Eq. (6) is used without further simplification. In its present form, it is inapplicable to cases where  $|v|$  approaches the sound speed, so that the pressure waves are always in the vicinity of the beam. Modifications to account for high velocities are easily accomplished [5] and could be included for future studies.

The laser beam is described by the scalar wave equation in the paraxial approximation. The derivation of this equation is detailed elsewhere [4] and is

$$2ik \frac{\partial \psi}{\partial z} + \frac{\partial^2 \psi}{\partial x^2} + \frac{\partial^2 \psi}{\partial y^2} + k^2(n^2 - 1)\psi = 0, \quad (9)$$

where  $\psi$  is the complex scalar wave amplitude (electric field  $E = \psi \exp[i(kz - \omega t)]$ ),  $k$  is the radian wavenumber  $2\pi/\lambda$ , and  $n(x, y, z, t)$  is the index of refraction, with its ambient value being taken to be  $n = 1$ . Equation (9) holds for slowly varying amplitude in the  $z$  direction,  $|k \partial \psi / \partial z| \gg |\partial^2 \psi / \partial z^2|$ . The intensity is  $C/8\pi |\psi|^2 e^{-\alpha z}$ . Equation (9) is coupled to Eq. (6) via the Lorentz-Lorentz law,

$$\frac{n^2 - 1}{n^2 + 2} = N\rho, \quad (10)$$

where  $N$  is the molecular refractivity

$$N = -\frac{2}{3} \frac{T_0}{\rho_0} \frac{\partial n}{\partial T} \quad (11)$$

for a perfect gas, ambient index equal to one, and small density changes  $\rho_1$ .

Note that the time dependence in Eq. (9) is implicitly contained in the change in index  $n^2 - 1$ . The high-frequency electric field oscillations have been removed, and the speed of light has been taken to be infinite (neglecting retardation). Thus the light beam is altered on a time scale determined by the fluid motion.

## COMPUTATIONAL DETAILS

Equations (6) (9), and (10) are solved in the following sequence (as given by the flowchart in the Appendix).

The amplitude appropriate for the aperture distribution of interest is given at  $z = 0$  for all  $t$ . Using these values the density change between  $z = 0$  and  $z = \Delta z$  is predicted via Eq. (6) and the index change via Eq. (10). The wave amplitude is propagated to  $z = \Delta z$ , all  $t$ , via Eq. (9), and this new intensity pattern is used to recalculate the index field to correct the amplitudes. This completes the basic iteration module from which a solution is constructed by marching from aperture to focus or range of interest.

The time integration in Eq. (6) must be treated with care. Since the integrand depends on the upper limit it appears that the integral must be recomputed completely at each time step. This can be avoided as follows: The density at  $t + \Delta t$  is, by definition

$$\rho(\mathbf{r}, z, t + \Delta t) = - \frac{(\Gamma - 1)\alpha_{abs}}{C_S^2} \int_0^{t + \Delta t} I[\mathbf{r} - \mathbf{v}(t + \Delta t - t'), z, t'] dt', \quad (12)$$

and we wish to relate it to  $\rho(\mathbf{r}, z, t)$ . We have

$$\begin{aligned} \rho(\mathbf{r}, z, t + \Delta t) &= - \frac{(\Gamma - 1)\alpha_{abs}}{C_S^2} \int_0^t I[\mathbf{r} - \mathbf{v}(t + \Delta t - t'), z, t'] dt' \\ &\quad - \frac{(\Gamma - 1)\alpha_{abs}}{C_S^2} \int_t^{t + \Delta t} I[\mathbf{r} - \mathbf{v}(t + \Delta t - t'), z, t'] dt' \\ &= \rho(\mathbf{r} - \mathbf{v}\Delta t, z, t) - \frac{(\Gamma - 1)\alpha_{abs}}{C_S^2} \int_t^{t + \Delta t} I[\mathbf{r} - \mathbf{v}(t + \Delta t - t'), z, t'] dt'. \end{aligned}$$

The integration can be done by trapezoidal rule to give

$$\rho(\mathbf{r}, z, t + \Delta t) = \rho(\mathbf{r} - \mathbf{v}\Delta t, z, t) - \frac{(\Gamma - 1)\alpha_{abs}}{C_S^2} [I(\mathbf{r}, z, t + \Delta t) + I(\mathbf{r} - \mathbf{v}\Delta t, z, t)] \frac{\Delta t}{2}. \quad (13)$$

We do not know  $I(\mathbf{r}, z, t + \Delta t)$  at this point in the calculation, since we need  $\rho(\mathbf{r}, z, t + \Delta t)$  to get it. Thus we estimate  $I(\mathbf{r}, z, t + \Delta t)$  from the time derivative

$$I(\mathbf{r}, z, t + \Delta t) \approx I(\mathbf{r}, z, t) + \Delta t \frac{\partial I}{\partial t}(\mathbf{r}, z, t) + \dots$$

We replace the time derivative by a central difference

$$\frac{\partial I}{\partial t} \rightarrow \frac{I(\mathbf{r}, z, t + \Delta t) - I(\mathbf{r}, z, t - \Delta t)}{2\Delta t};$$

thus,

$$I(\mathbf{r}, z, t + \Delta t) \cong 2I(\mathbf{r}, z, t) - I(\mathbf{r}, z, t - \Delta t).$$

Finally,

$$\begin{aligned} \rho(\mathbf{r}, z, t + \Delta t) = & \rho(\mathbf{r} - \mathbf{v}\Delta t, z, t) - \frac{(\Gamma - 1)\alpha_{abs}}{C_S^2} [2I(\mathbf{r}, z, t) \\ & - I(\mathbf{r}, z, t - \Delta t) + I(\mathbf{r} - \mathbf{v}\Delta t, z, t)] \frac{\Delta t}{2}. \end{aligned} \quad (14)$$

### FREE CONVECTION

For beams propagating in the atmosphere, the buoyancy induced by laser heating can be neglected [3]. In laboratory simulations, however, free convection can produce significant flow of absorber in a time comparable to the transient heating period of thermal blooming. Buoyancy should not be ignored in the experiments used to check the computer code and in the following discussion. Thus a calculation of the induced vertical velocity was incorporated in the code in order to achieve a satisfactory quantitative confirmation of the computer calculation.

Therefore, in addition to Eq. (5), we must also solve, neglecting viscosity,

$$\rho_0 \left( \frac{\partial v_B}{\partial t} + \mathbf{v} \cdot \Delta v_B \right) = \rho_1 g, \quad (15)$$

where  $g$  is a negative number, representing the acceleration of gravity. The solution to Eq. (15) is

$$v_B(x, y, t) = \frac{g}{\rho_0} \int_0^t \rho_1 [x - v_X(t - t'), y - v_B(t - t'), t'] dt'. \quad (16)$$

And due to the presence of a vertical component of velocity, Eq. (6) becomes

$$\rho_1(x, y, t) = \frac{-(\Gamma - 1)\alpha}{C_S^2} \int_0^t I[x - v_x(t - t'), y - v_B(t - t'), t'] dt'. \quad (17)$$

Combining Eqs. (15) and (16) and integrating by parts gives

$$v_B = \frac{g\rho_1 t}{\rho_0} + \frac{g(\Gamma - 1)\alpha}{\rho_0 C_S^2} \int_0^t t' I[x - v_x(t - t'), y - v_B(t - t'), t'] dt'. \quad (18)$$

The computer code must solve Eqs. (17) and (18) simultaneously. This is accomplished by alternating the calculation of  $\rho_1$  and  $v_B$  and iterating until each converges. In practice, it was found that one iteration was sufficient. The algorithm for calculating  $v_B$  is similar to the method used for  $\rho_1$  and given in Eq. (14). Define

$$J(x, y, t) = \frac{g(\Gamma - 1)\alpha}{\rho_0 C_S^2} \int_0^t t' I[x - v_x(t - t'), y - v_B(t - t'), t'] dt'; \quad (19)$$

then the algorithm is

$$\begin{aligned} v_B(x, y, t + \Delta t) = & \frac{g\rho_1(t)}{\rho_0} (t + \Delta t) + J(x - v_x \Delta t, y - v_B \Delta t, t) \\ & + \frac{g(\Gamma - 1)\alpha}{\rho_0 C_S^2} \frac{\Delta t}{2} \left\{ (t + \Delta t) [2I(x, y, t) - I(x, y, t - \Delta t)] \right. \\ & \left. + tI(x - v_x \Delta t, y - v_B \Delta t, t) \right\}, \end{aligned} \quad (20)$$

and Eq. (14) becomes

$$\begin{aligned} \rho_1(x, y, t + \Delta t) = & \rho(x - v_x \Delta t, y - v_B \Delta t, t) \\ & - \frac{(\Gamma - 1)\alpha}{C_S^2} \frac{\Delta t}{2} [2I(x, y, t) - I(x, y, t - \Delta t) \\ & + I(x - v_x \Delta t, y - v_B \Delta t, t)]. \end{aligned} \quad (21)$$

These algorithms require the storage of two earlier values of the intensity field,  $I$ , one earlier value of the integral  $J$  and the current values of  $v_B$  and  $\rho$ .

Earlier in this section it was stated that the equations for the conservation of mass and energy would be solved in the isobaric limit. This will now be justified by considering the time scales of importance in the experiment which was used to provide validation of the computer code [6]. A pivoting gas absorption cell provided a null convection point requiring a full four-dimensional analysis (Fig. 1). The appropriate time interval for use in the computations follows from these considerations.

In setting up the requisite hydrodynamic equations to solve the propagation problem, one can take advantage of the large difference between time scales characterizing pressure-wave transients and convective effects. The former travel at the speed of sound and are therefore lost from the beam region in a time like  $a(z)/c_s$ , which is about  $10 \mu\text{s}$  for these experiments. The origins of convection effects are twofold: (1) the relative velocity between gas and laser beam due to pivoting of the cell and (2) the induced buoyancy due to the heating of the gas. To compare the time scale, due to cell pivoting with the pressure equilibration time calculated, we chose the maximum velocity induced by pivoting in all of experiments used for comparison. This occurred when the cell was pivoted about the point  $z = -10 \text{ cm}$  with a slew rate of  $0.2 \text{ rad/s}$ , giving a characteristic time (at the beam waist) of  $3.63 \text{ ms}$ . All other velocities at different slew rates, ranges, and pivot points are slower. Thus the forced convection times are at least three orders of magnitude slower than the time characteristic of the pressure effects. The buoyancy-induced velocities were estimated and found to be greater than  $0.04 \text{ s}$ , and therefore comparable to thermal-blooming decay times.

The time scale of the various hydrodynamic phenomena suggests that we can ignore sound effects and solve merely the simpler problem. Beam degradation is taken to be and was found to be negligible during sound transit times. In addition, the effects of the pressure waves striking the wall of the gas cell and returning to the region of the beam are ignored and were suppressed in the experiment by suitable choice of all walls.

Great care was taken to model the experiment as closely as possible. The beam was propagated without absorption from  $z = 0$  to  $z = 80 \text{ cm}$ . At  $z = 80 \text{ cm}$  the absorption coefficient assumed the value  $0.42 \text{ m}^{-1}$ . The absorption was dropped to zero at  $103 \text{ cm}$  farther on, and the final values were calculated  $10 \text{ cm}$  beyond this point. The nominal beam sizes of  $0.32 \text{ cm}$  and  $0.08 \text{ cm}$  at entrance and exit could not be achieved with diffraction-limited unperturbed propagation. Hence, wavelength scaling was used to produce a focal spot  $1.43$  times the diffraction limit to fit the beam-size constraint. A computational "detector" was used by counting the flux at mesh points which fell inside the circle with radius equal to the radius of the experimental detector. Thus the code could give in principle an absolute comparison with the experiment. For the purposes of this work, however, all flux values were divided by the initial value to produce data similar to that taken experimentally. The computational detector was made to sense the peak intensity point and followed it in the horizontal cell model. The detector remained on-axis.

The necessity to introduce natural convection into the code became apparent when the horizontal experiment was modeled without natural convection. The data indicated too much heating gas in the computational model and suggested the presence of another cooling mechanism beside the forced convection. The hydrodynamics were then altered to produce the algorithm in the preceding discussion.

## SOURCES OF ERROR

The following approximations have contributed to the inaccuracy of the code results:

- Wavelength scaling to account for nondiffraction-limited behavior. This gives results that are most likely slightly high.

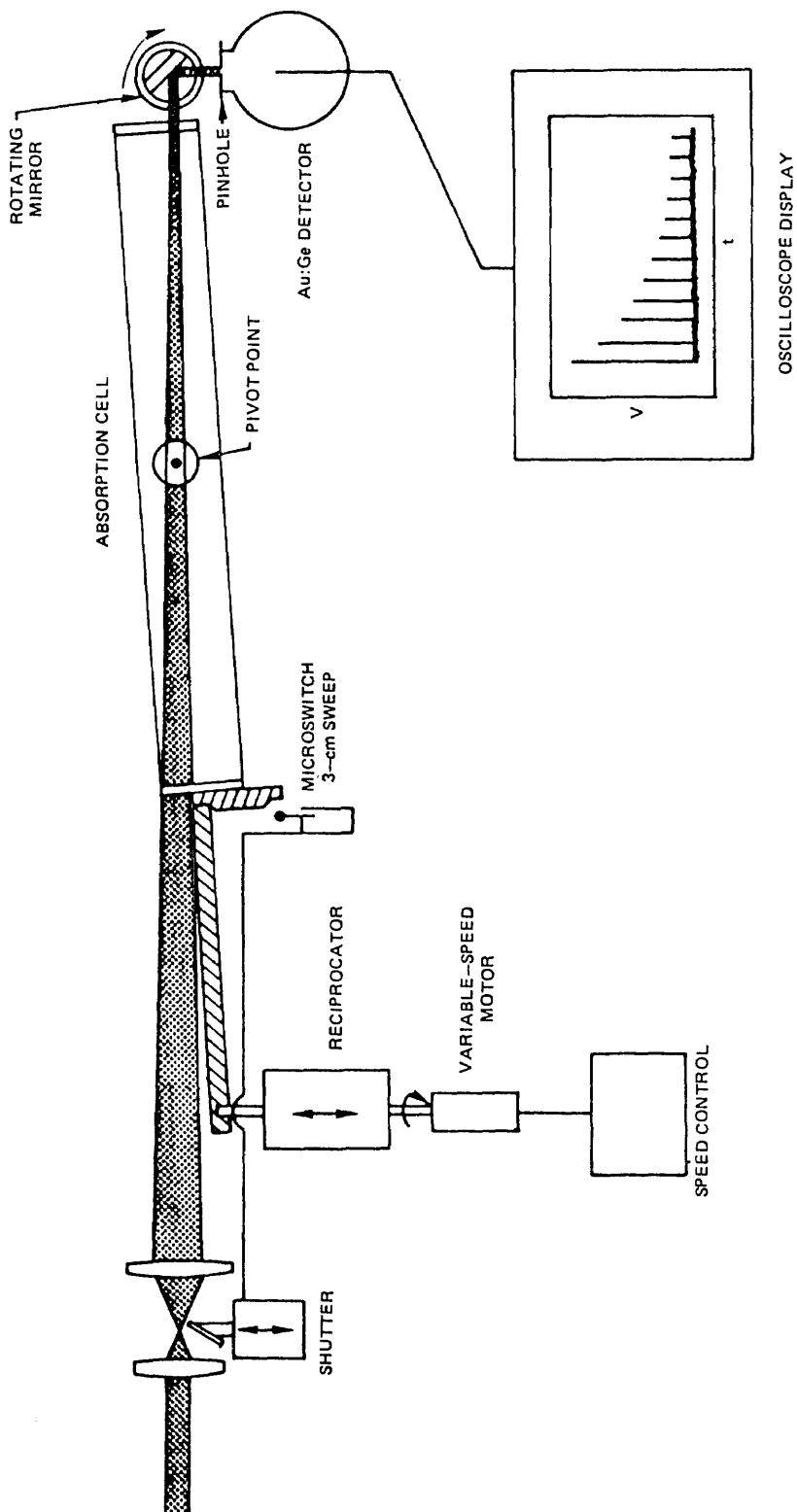


Fig. 1—Experimental arrangement

- Coarse discretization in  $x$ ,  $y$ , and  $z$  to avoid long running times. This can give answers either too high to too low.
- Coarse discretization in  $t$  coupled with crude (trapezoidal rule) time integration. The direction of this error is unknown.
- Use of only one iteration in solving Eqs. (14) and (15). This leads to an underestimate of  $v_B$  and thus lower results than if enough iterations for convergence were used.
- The approximation of Eqs. (17) and (18). This is a predictor without a corrector, and since  $\partial I/\partial t < 0$ , it gives rise to a lower value of  $I$ . Lower values of  $I$  will give smaller density changes and smaller buoyancy velocities which tend to cancel to order  $\Delta t$ .

If one assumes all of these effects to be random and at most 10%, one can account for an rms error of about  $\pm 5\%$ , and the computer-generated points should be taken to fall within these error bounds.

## COMPARISON WITH EXPERIMENT

In the experiment [6], a  $\text{CO}_2$  laser beam of nominal 10-W power was passed through an absorbing cell which had the capability of being pivoted. The pivot point was variable. If  $z_s$  is the position of the pivot point, then the forced convection at any range  $z$  is given by

$$v_x = (z - z_s)\Omega, \quad (22)$$

where  $\Omega$  is the pivot rate. If the pivot point is inside the absorbing cell, there is no forced convection at that point, and buoyance develops as the sole heat removal agent. The experiment provided a good test of the computer calculation.

Figures 2 through 7 are plots of the relative intensity as a function of time for pivot points varying from  $z_s = -45$  cm to  $z_s = 90$  cm, with  $z = 0$  taken at the entrance of the 1-meter cell. The relative intensity is defined as

$$I_{rel}(t) = I_{meas}(t)/I_{vac}e^{-\alpha L}, \quad (23)$$

where  $I_{vac}$  is the reference level obtained with the cell evacuated,  $\alpha$  is the absorption coefficient of the gas absorber, and  $L$  is the length of the cell. The solid points are experimental, and the open points are obtained from the four-dimensional code. The agreement is quite good in all cases. Improvement could be achieved by finer sampling of the calculation in range, especially in the vicinity of a pivot point within the cell. Since the code calculations are already quite time consuming, further refinements were not warranted in view of the satisfactory results obtained. This agreement is close enough for the purposes for which the code was developed.

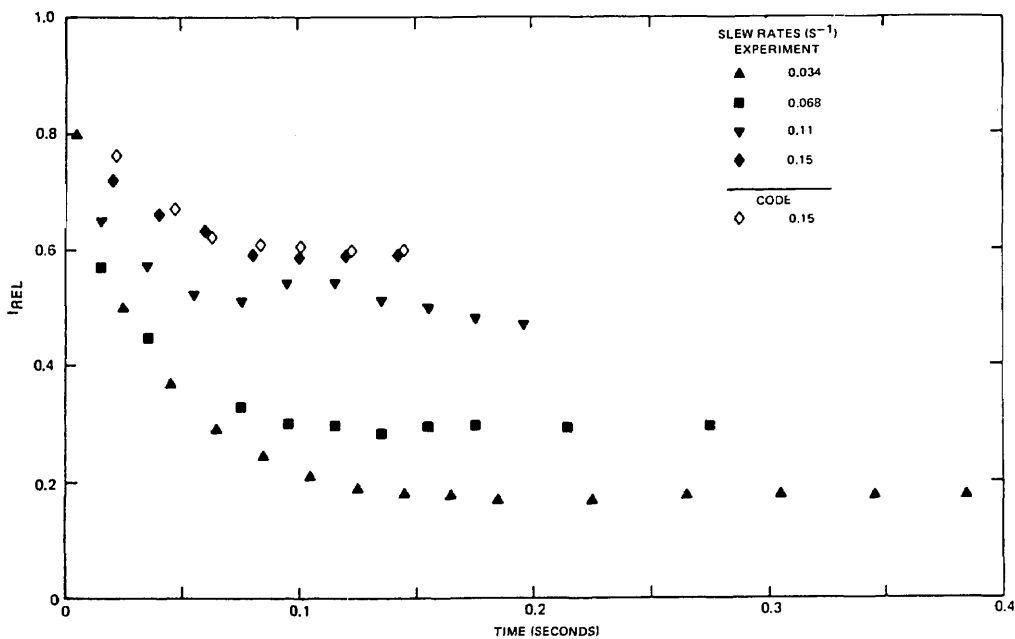


Fig. 2— $I_{rel}$  vs  $t$  for  $z_s = -45$  cm

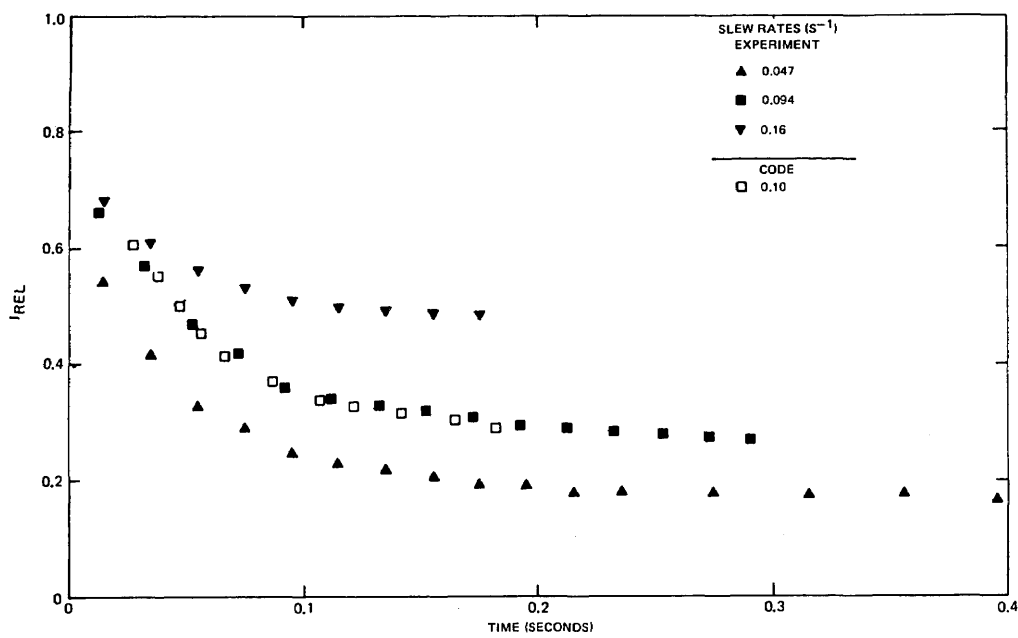


Fig. 3— $I_{rel}$  vs  $t$  for  $z_s = -10$  cm

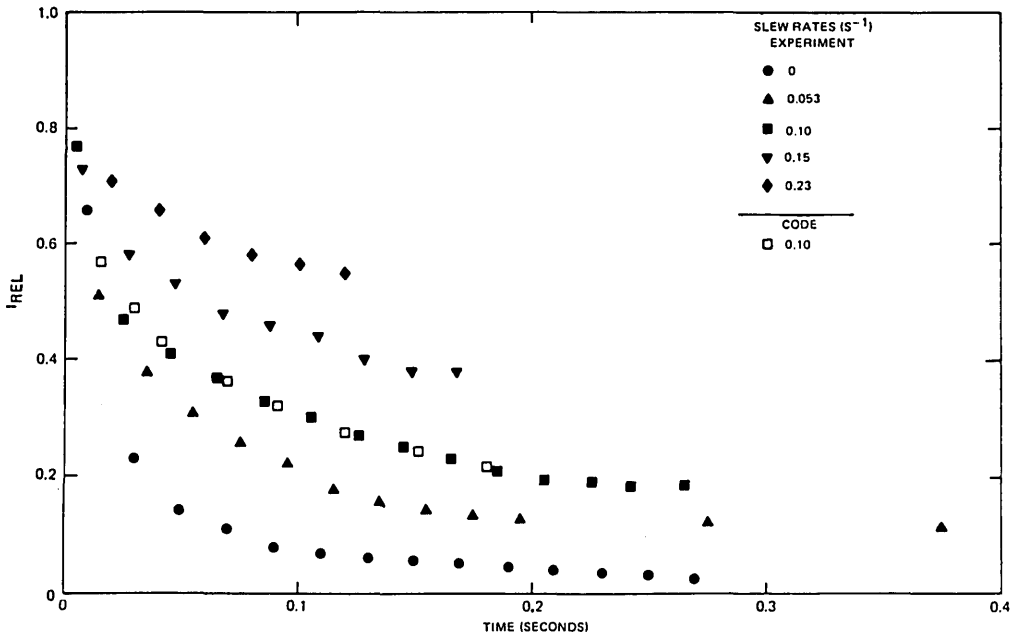


Fig. 4— $I_{rel}$  vs  $t$  for  $z_s = 0$

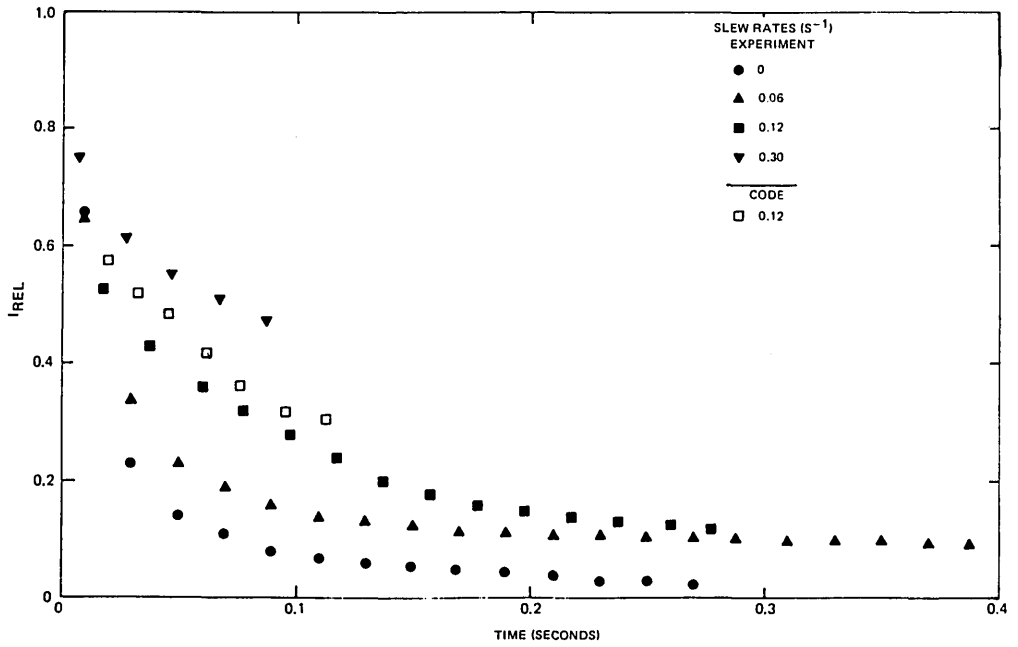


Fig. 5— $I_{rel}$  vs  $t$  for  $z_s = +10$  cm

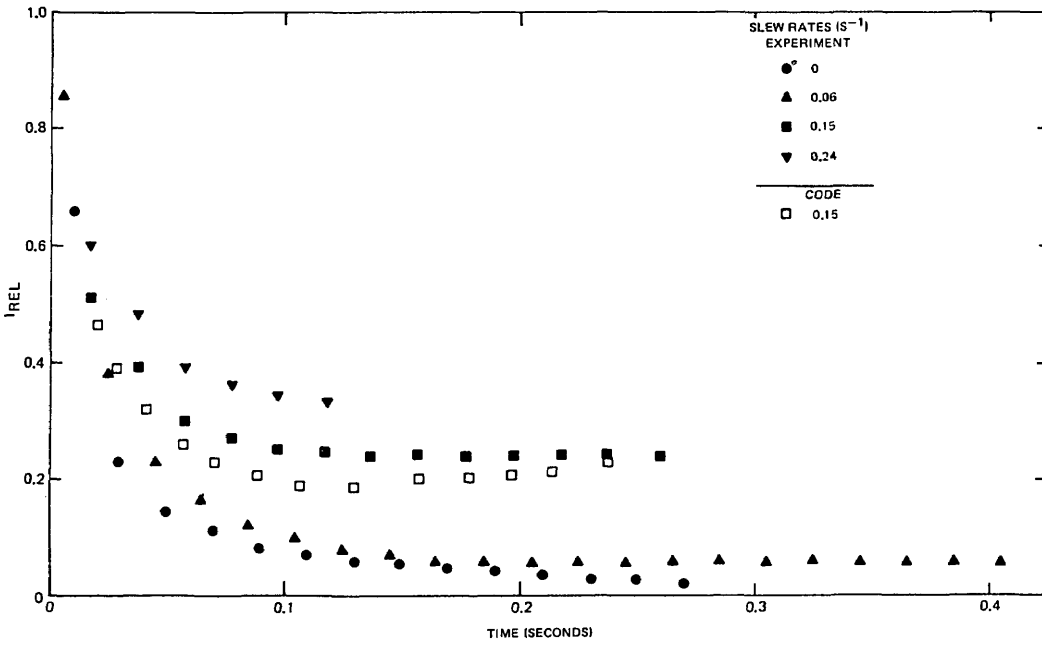


Fig. 6— $I_{rel}$  vs  $t$  for  $z_s = +50$  cm

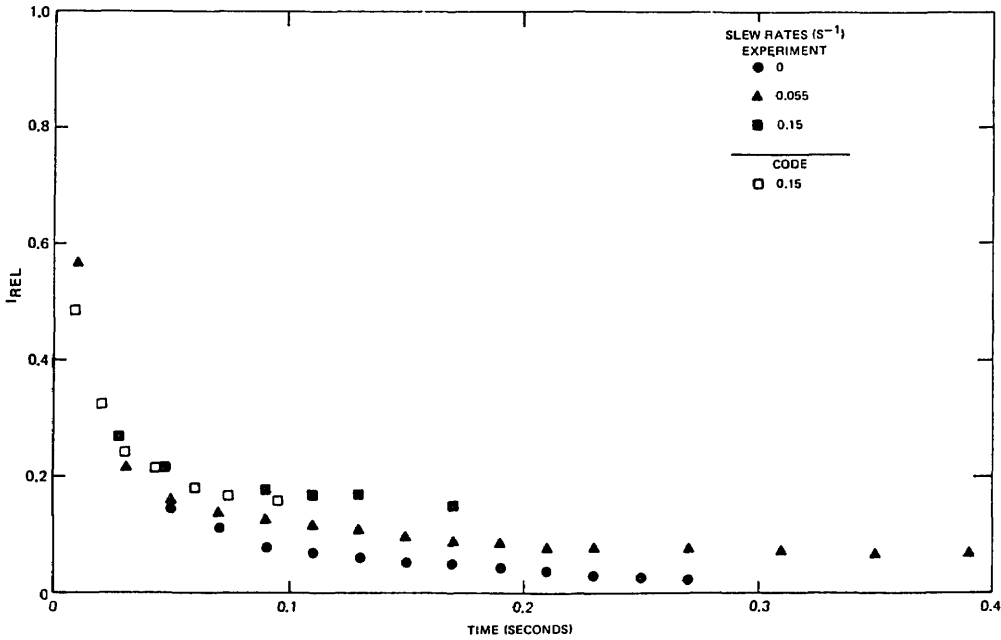


Fig. 7— $I_{rel}$  vs  $t$  for  $z_s = +90$  cm

## CONCLUSIONS

A four-dimensional computer code has been written which solves for the propagation of an intense laser beam passing through an absorbing fluid. Included are the calculations of complex hydrodynamic flows induced by the beam itself. The code was confirmed by comparing its results with those of an experiment. This comparison required (for agreement) that the code include all features of the interaction of beam and absorber on each other in a self-consistent way.

## REFERENCES

1. P.B. Ulrich, "Numerical Methods in High Power Laser Propagation" and J.N. Hayes, "High Power Laser Propagation: An Overview", in the Proceedings, on the Conference on "Optical Propagation in the Atmosphere" by the Electromagnetic Propagation Panel of the Advisory Group for Aerospace Research and Development (AGARD) of NATO, held at the Technical University, Lyngby, Denmark Oct 1975.
2. P.B. Ulrich, J.N. Hayes, and A.H. Aitken, *Journal of Optical Society of America* **62**, 298 (1972)
3. J.N. Hayes, *Applied Optics* **11**, 455, (1972)
4. A.H. Aitken, J.N. Hayes, P.B. Ulrich, NRL Report 7293, May 1971; Available from National Technical Information Service, No. AD725111.
5. J.N. Hayes *Applied Optics* **13**, 2072 (1974); J.A. Fleck, J.R. Morris, M.J. Feit, UCRL Report 51826, June 1975.
6. R.T. Brown, P.J. Berger, and F.J. Gebhardt, UARL Report N921724-7, February 1974 and UARL Report N921724-12, October 1974.

## Appendix

### FLOWCHART

